Asian Journal of Chemistry; Vol. 32, No. 10 (2020), 2624-2632

ASIAN JOURNAL OF CHEMISTRY

https://doi.org/10.14233/ajchem.2020.22815

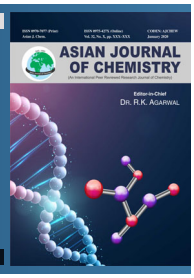

Adsorption of Cr(VI), Pb(II) Ions and Methylene Blue Dye from Aqueous Solution using Pristine and Modified Coral Limestone

C.S. NKUTHA*, N.D. SHOOTO and E.B. NAIDOO

Applied Chemistry and Nano Science Laboratory, Department of Chemistry, Vaal University of Technology P.O. Box X021, Vanderbijlpark 1900, South Africa

*Corresponding author: E-mail: cynthiankutha61@gmail.com

Received: 5 May 2020; *Accepted*: 28 July 2020; *Published online*: 25 September 2020; AJC-20080

This work reports the feasibility of using pristine and chemically modified coral limestones by acid and base. Their potential adsorptive capabilities is probed by treatment of toxic Cr(VI), Pb(II) ions and methylene blue in aqueous solution under different experimental parameters by batch method. Parameters such as agitation time, concentration, temperature and pH were varied to understand the sorption behaviour of the adsorbents in each case. The adsorbents were characterized by SEM, XRD and FTIR. Morphological analysis by SEM micrographs show that the surface of all adsorbents was irregular in nature. XRD spectra confirmed the orthorhombic structure of aragonite in the pristine coral limestones (PCL), acid modified coral limestones (ACL) and base modified coral limestones (BCL). FTIR results affirmed the presence of (CO_3^{2-}) and (-C=O) groups of the carbonate ions and Ca-O attachment to the surface of PCL and removal of $CaCO_3$ characteristic peaks in ACL and BCL. However, in the modified adsorbents shifting of Ca-O peaks occurred. The recorded maximum adsorption capacities of PCL, ACL and BCL for Cr(VI) ions were 69.42, 65.04, 64.88 mg/g, Pb(II) ions 39.36, 74.11, 78.34 mg/g and methylene blue 37.24, 46.28, 46.39 mg/g, respectively. The uptake of Pb(II), Cr(VI) ions, methylene blue onto PCL fitted Freundlich model. Also the uptake of Cr(VI) ions and methylene blue onto ACL and BCL fitted Freundlich isotherm. However, uptake of Pb(II) ions onto both ACL and BCL fitted Langmuir isotherm. The data revealed that the adsorption of Pb(II) ions onto PCL and ACL and methylene blue dye onto PCL was exothermic. Whilst the adsorption of Cr(VI) ions onto PCL, ACL and BCL and methylene blue dye onto ACL and BCL were endothermic in nature, hence increasing the temperature would enhance the uptake of Pb(II) ions onto BCL, Cr(VI) ions onto ACL and BCL and methylene blue onto ACL and BCL. The obtained (ΔG^o) values at all studied temperatures for the adsorption of Pb(II), Cr(VI) ions and methylene blue onto PLC, ACL and BCL indicated a spontaneous process.

Keywords: Pristine, Modified coral limestone, Cr(VI), Pb(II), Methylene Blue, Adsorption.

INTRODUCTION

Water contamination across the globe has consistently become a growing environmental issue. This has been due to expanding economies which has led to an increase in industrial activity, growth and urbanization [1]. The diversification of anthropogenic activities has led to the prevalence of toxic pollutants in fresh water bodies which is persistent and irreversible [2]. The discharge of untreated effluents into the various industrial works such as pulp & paper, tanning, textiles, cosmetics and others, causes the widespread of toxic pollutants such as metals and dyes [3,4].

These toxic pollutants degrade the environment and when they come into contact with humans they introduce potential health hazards. The primary route of entry into the human body is through food and water. The ions of these toxic pollutants have detrimental effects even at low concentration [5]. They interfere, block, replace and poison many aspects of biosynthesis [6]. Generally, toxic metal and dye pollution is persistent and irreversible [2].

Various treatment technologies have been employed to address the widespread contamination of water and wastewater. These methods include adsorption [7], ion-exchange [8], membrane separation [9], electrocoagulation [10], solvent extraction and catalytic degradation [11]. Of these technologies, adsorption has been found to be more beneficial in application because it is inexpensive, highly efficient in low and high concentration removal, simple in operation and a widespread of adsorbents can be used [12].

Various porous materials have been used as adsorbents, such as activated carbon, activated coal, activated silica, mesoporous carbon, nanostructured carbon [9] and pristine graphene and its oxide [13]. They have been considered as effective because of their excellent characteristics such as their large surface area, excellent chemical stability and geometrical structure of pores. These commercially available adsorbents applied for the remedial action of the high accumulation of toxic pollutants in water are unviable in that they are expensive to use and maintain, therefore providing difficulty in scaling up for industrial use [10].

Recently scientists have explored the use of biomass in the form of agricultural waste, natural materials and solid waste. The use of biosorbents such as bamboo charcoal [11], *Ficus carica* bast [4], beach sand [14], macadamia nutshells [15], *Nigella sativa* [16], mucuna beans [17], cow dung [1] and banana peel [18] have been studied. The materials are not selective in their removal, abundant in nature, inexpensive and show high removal capacity in both their pristine and modified nature for both metals and dyes.

Solid waste from agriculture, households and the ocean has been highlighted as being important due to their potential applications in the fourth industrial revolution as valuable recyclable waste for various applications. Solid waste washed up from the ocean that is made up of calcerous materials such as oyster shells, crab shells, mussel shells and coral limestones is of significance especially because the main component of their shell structure is $CaCO_3$ which is one of the most abundant minerals on the surface of the earth. The formation of these valuable materials sterms from the process of carbon capture in the ocean and their main constituent is calcium ions, which has been reported to have the capability to immobilize toxic pollutants [2].

Coral limestone are the calcerous remains of the hard corals which can be found on the beach shores of many coral bearing beaches. They are used as decorative artifacts, prehestoric banks of environmental conditions and bio-detectors for anthropogenic activities related to industrial activities [19,20]. Coral limestones can be easily broken when storms occur, hence their abundance on the shore of reef containing sites.

Very few documents have reported on the use of coral limestones as potential adsorbents for removing pollutants from water. Shookohi *et al.* [21,22] studied the removal of Pb(II), Cd(II) ions and acid cyanine 5R dye. Nourozi *et al.* [23] reported on the sorption of arsenate(V) ions. Malakootian *et al.* [24] studied the adsorptive behaviour of red 198 from textile wastewater. Currently coral limestones adsorption studies scope is too limited. To the best of our knowledge no study until now has explored acid and base treated coral limestone as potential adsorbents and no literature was found which reports on the adsorption of Cr(VI) ions and methylene blue by coral limestones. Therefore, to our best of knowledge, this study is the first of its kind to report on modified ACL and BLC limestones for the removal of Pb(II), Cr(VI) ions and methylene blue.

EXPERIMENTAL

Coral limestones were obtained from Wolmar public beach as washed up waste on the shore in Flic en Flac, Mauritius. Hydrochloric acid (HCl)–32%, sodium hydroxide (NaOH) pallets–98.5% A.R grade, methylene blue ($C_{16}H_{18}N_3SCl$)–95% A.R grade, chromium dichromate ($K_2Cr_2O_7$)–99.9%, lead nitrate ($Pb(NO_3)_2$)–99.5% were purchased from Merck South Africa LTD.

Preparation of the adsorbent

Preparation of pristine coral limestones: The coral limestone was washed with deionized water under agitation at 200 rpm for 30 min to remove sand and debris. The adsorbent was crushed using a grinder to a fine grainy powder, the powdered sample was further washed under rotation at 40 °C in de-ionized water. The powdered sample was dried at 75 °C overnight and labelled pristine coral limestone (PCL).

Preparation of acid modified coral limestones: PCL sample was subjected to washing and drying at 75 ºC. The PCL was then dispersed in 0.05 M HCL solution for a period of 60 min while stirring. The sample was dried overnight at 75 °C in an oven and labelled as ACL.

Preparation of base modified coral limestones: PCL sample was subjected to washing and drying at 75 ºC. The PCL was then dispersed in 0.1 M NaOH solution for a period of 60 min while stirring. The sample was dried overnight at 75 ºC in an oven and labelled as BCL.

Adsorption experiments: Adsorption studies of the PCL, ACL and BCL were done in batches by varying parameters such as agitation time (5, 10, 15, 20, 30, 40, 60, 90 and 120 min), concentration (20, 40, 60, 80, 100, 120. 140, 160, 180 and 200 mg/L), pH (2, 4, 6, 8 and 10) and temperature (289, 299 and 309 K). The adsorbents mass was kept constant at 100 mg for PCL and 50 mg for ACL and BCL and stock solutions of 1000 mg/L were prepared. From the prepared stock solutions of Pb(II), Cr(VI) and methylene blue, working standards of 100 mg/L were prepared. Adsorption was carried out in a 50 mL centrifuge tube with 20 mL of solution added, under agitation at 200 rpm. After each experiment, the respective centrifuge bottles were removed and centrifuged for 5 min at 4000 rpm. The supernatants were analyzed using AAS and UV, respectively.

Data analysis: The adsorption capacities (q_e) (mg/g) of PCL, ACL and BCL towards Cr(VI), Pb(II) and methylene blue were evaluated by eqn. 1, where C_o and C_e are the initial and final concentrations of Cr(VI), Pb(II) and methylene blue in the solution in (mg/L); V is the volume of the solution (mL) and m is the mass of the adsorbents (g).

$$q_e = \frac{(C_o - C_e)V}{m} \quad (1)$$

Kinetics, pseudo-first order (PFO), pseudo-second order (PSO) and intra-particle diffusion (IPD) models were evaluated by eqns. 2, 3 and 4, respectively. On PFO and PSO equations, (q_e) is the amount of total Cr(IV), Pb(II) and methylene blue adsorbed in (mg/g) at time (t). PFOM rate constant (k_1) in (min^{-1}) and PSOM rate constant (k_2) in (g/mg min). IPDM rate constant (k_i) in (g/g min). (C) is the amount of Cr(VI), Pb(II) and methylene blue on the adsorbent surface. Kinetic models were evaluated by nonlinear equations introduced into KyPlot software:

$$q_e = q_t(1 - e^{-k_1 t}) \quad (2)$$

$$q_e = \frac{1 + k_2 q_e t}{k_2 q_e^2 t} \quad (3)$$

$$q_t = k_i(t^{1/2}) + C \quad (4)$$

Adsorption isotherms (Langmuir and Freundlich models) were evaluated by eqns. 5 and 6, respectively. Langmuir, parameter (Q_o) is the maximum adsorption capacity of the adsorbent in (mg/g), (b) is the solute surface interaction energy constant. Freundlich, (k_f) is the capacity factor constant and (1/n) is the isotherm linearity parameter constant.

$$q_e = \frac{Q_o b C_e}{1 + bC_e} \quad (5)$$

$$q_e = k_f C_e^{1/n} \quad (6)$$

Enthalpy change (ΔH°), entropy change (ΔS°) and free energy change (ΔG°) were evaluated by eqns. 7 and 8 at 289, 299 and 309 K.

$$\ln K_c = \frac{\Delta H^\circ}{RT} - \frac{\Delta S^\circ}{R} \quad (7)$$

$$\Delta G^\circ = -RT \ln K_c \quad (8)$$

K_c is the equilibrium constant of thermodynamic function. K_c values were calculated by means of eqn. 9:

$$K_c = \frac{q_e}{C_e} \quad (9)$$

Characterization: The PCL, ACL and BCL were affirmed by SEM, FTIR and XRD techniques. Scanning electron microscopy (SEM) images were taken on a Nova Nano SEM 200 from FEI operated at 10.0 kV. Fourier transform infrared spectrometer (FTIR/FTNIR) from Perkin Elmer was used to determine the functional groups. X-ray diffractometry (XRD-7000, Shimadzu, Japan) was used to analyse the diffraction patterns. UV-Vis analyses were performed with a double beam spectrometer-Perkin Elmer Lambda 25 UV/Vis, which collects spectra from 180-1100nm. UV and visible range using a slit of 1.0 and width of 0.1. A lamp of tungsten and deuterium were used to provide illumination, using flame atomic absorption spectrophotometer (Shimadzu AA-7000, Japan). Point zero charge was done using an orbital shaker for 24 h, using the drift method and sodium nitrate salt.

RESULTS AND DISCUSSION

SEM analysis: The SEM images of the PCL, ACL and BCL are shown in Fig. 1a-f. The above SEM images were used to study the surface of the adsorbents, it was observed that the surface morphology was irregularly shaped in Fig. 1a-b for PCL showing a surface morphology which is made up of a multicomponent network of grains assembled in a continuous matrix having an amorphous shape. Previously Galván-Ruiz *et al.* [25] noted similar surface distribution morphology, which appears like it was made up of attached particles onto the surface. However, this trend in the morphology disappears on the modified coral limestone. Fig. 1c-f for ACL and BCL show an irregular surface morphology, which is made up of a compact structure with angular grains for the modified coral limestone. The surface of ACL Fig. 1c-d shows a rougher textural surface, which can be attributed to the incomplete detachment of CO_3^{2-} and removal of calcite. The surface morphology for the BCL Fig. 1e-f is more compact, whereby the grainy surface from the PCL has been removed. This can also be confirmed by the FT-IR and XRD of the BCL, with removal of the CO_3^{2-} ions and the transition to the less metastable crystal structure of aragonite. The same surface morphology was observed by Du *et al.* [25] for the aragonite adsorbent, which was later confirmed by their XRD analysis.

FTIR analysis: The -IR spectra show the functional groups on the surface of PCL, ACL and BCL as shown in Fig. 2. The sharp peak at 1459 cm^{-1} on the PCL corresponds to the asymmetric stretching of the C–O of carbonate ion (CO_3^{2-}). The low peak at 1785 cm^{-1} corresponds to the C=O of carbonate ion (CO_3^{2-}), the band was also observed in $CaCO_3$ sample, it was noticed that the intensity of the band to the standard was lower. The doublet peaks at 700 and 713 cm^{-1} are assigned to the Ca-O [26]. However, in ACL charasteristic peaks of Ca-O remained, but the intensity of the peaks was lower. It was observed that some peaks which are characteristic of $CaCO_3$ were removed and new peaks were obseved in the region 500 to 700 cm^{-1} which are characteristic of the attachment of a halogen on the ACL proving that modification was successful. The IR of ACL also revealed a shifting of Ca-O peaks in contrast to PCL at 460 and 404 cm^{-1}. The IR of BCL shows an intense characteristic peak of Ca-O at 404 cm^{-1}. This peak is shifted according the IR of PCL at 447 cm^{-1} and Balmain *et al.* [27] who obtained a broad peak at 450 cm^{-1}.

XRD analysis: The XRD of the PCL (Fig. 3a) revealed a mineral phase which is characteristic of the aragonite polymorph of the calcium carbonate mineral form. The crystalline phase of PCL has a characteristic doublet wavelength in the range 2θ = 26-27° [20], which suggests an armophous phase of the PCL. The diffraction patterns were found to be slightly shifted from those found in literature, a weak diffraction peak at 2θ = 29.6° was observed. This is attributed to the polymorphic transition of aragonite into calcite which may be due to grinding during sample preparation as this action causes heat, as mentioned by Balmain *et al.* [27] in their XRD results due to their sample preparation. Treatment of the PCL by acid and base saw the removal of the weak diffraction peak at 2θ = 29.6º, the mineral phase of ACL and BCL was still in the orthorhombic aragonite polymorphic phase (Fig. 3b-c). However, it was noticed that the mineral geochemistry of the coral matrix has been slightly altered in that the intensity of the diffraction peaks has decreased.

Physio-chemical analysis

Zero point charge studies: The $pH_{(PZC)}$ of PCL value was established at 7.6, which can be expected due to the carbonate (CO_3^2) ions characteristic as a neutralizing agent. The modified coral limestone ACL and BCL $pH_{(PZC)}$ were established at 9.7 and 8.3, respectively. The modification of the PCL with an acid and base saw the removal of (CO_3^{2-}) ions from the surface of the material. Thus the dominating charge of the neutral ionic

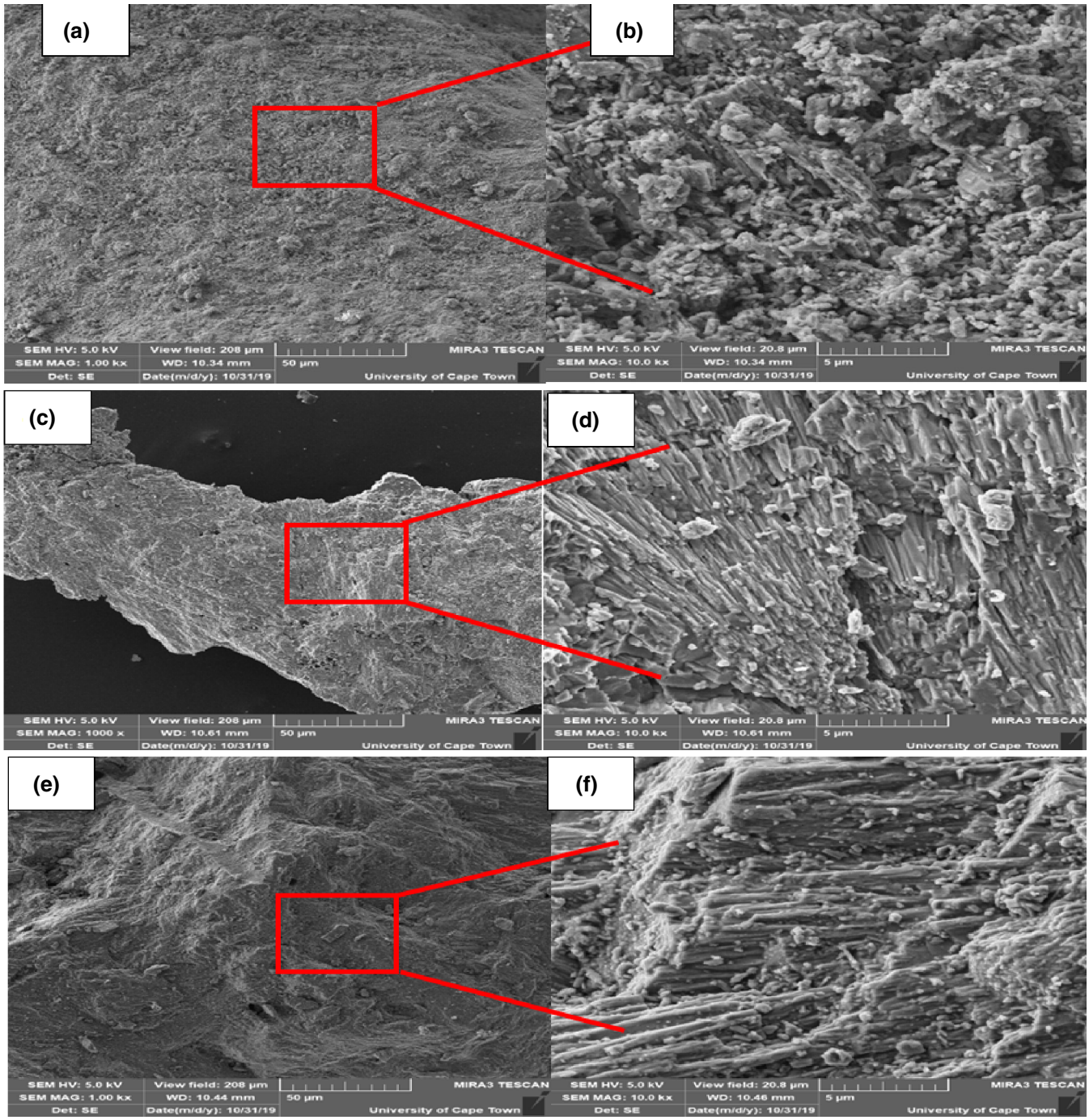

Fig. 1. SEM image of (a-b) PCL, (c-d) ACL and (d-e) BCL

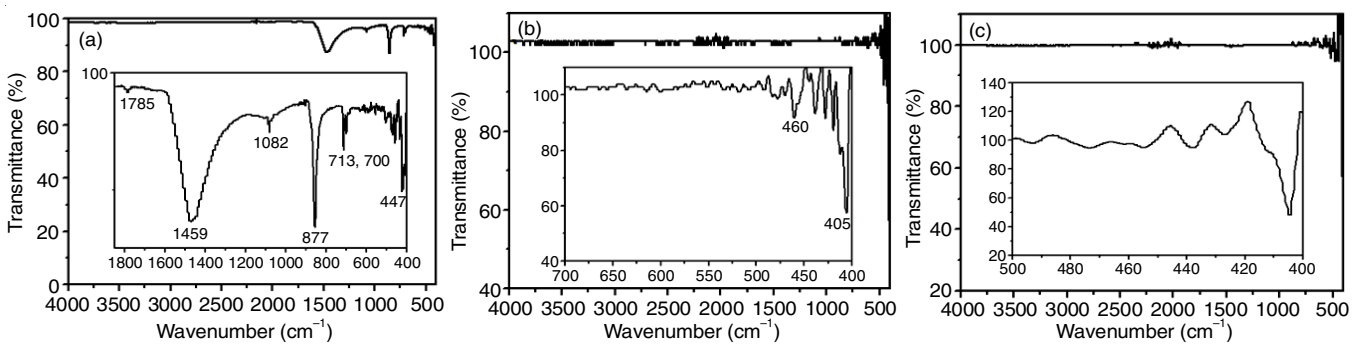

Fig. 2. IR spectra of (a) PCL (b) ACL (c) BCL

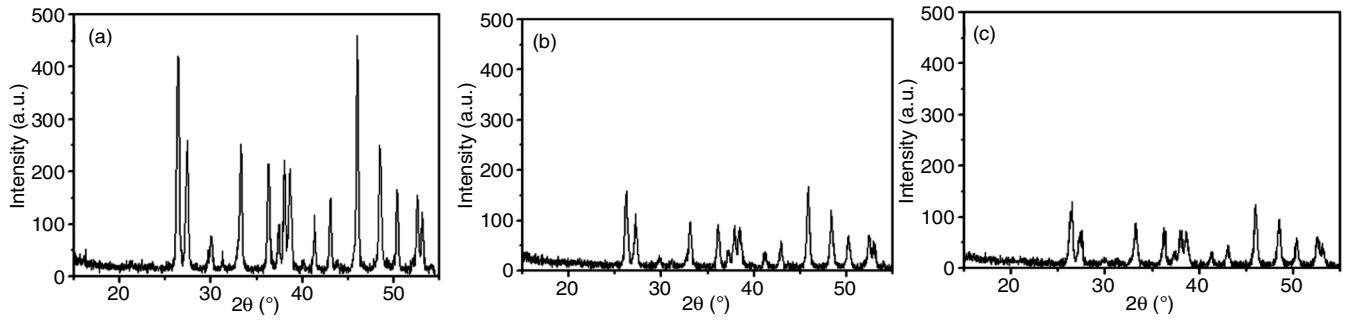

Fig. 3. XRD analysis (a) PCL, (b) ACL and (c) BCL

surface of PCL has been protonated and the surface is dominated by positively charged surface functionalities.

Adsorption studies

Effect of agitation time: The removal rates of methylene blue, Pb(II) and Cr(VI) ions by PCL, ACL and BCL was investigated at time intervals (5-120 min) as shown in Fig. 4a-c. In Fig. 4a, it was observed that the adsorption of methylene blue, Pb(II) and Cr(VI) ions onto PCL was fast within the interval 5-60 min, thereafter little to no adsorption was noted. Fast adsorption within the interval 5-60 min could be attributed to abundant active sites on the adsorbent surface however, beyond 60 min the active sites are occupied thus the adsorption is slowed down. This is atrributed to the difficulty of the species in solution to penetrate into the active sites and been repelled by the already adsorbed species onto the surface of PCL. It was observed that PCL had higher uptake for Cr(VI) than Pb(II) ions and methylene blue. Adsorption rates of ACL and BCL in Fig. 4c, were more or less the same. It was noted that both adsorbents had higher uptake for methylene blue than Cr(VI) and Pb(II) ions. The sorption was rapid in the initial stages thereafter it slowed down.

Kinetic analysis: The effect of agitation time data was subjected to generate kinetic data with which it was used to better understand the plausible adsorption mechanisms involved during the processes. The fitted kinetic models are non-linear pseudo-first order (PFO) and pseudo-second order (PSO) the obtained data is shown in Table-1. The correlation coefficient (r^2) values were evaluated and used to estimate the fitted kinetic model. The data revealed that adsorption of Pb(II) ions onto PCL had greater (r^2) value of 0.994 for PSO whilst Cr(VI) ions well fitted PFO with (r^2) values of 0.578. It was also found that the adsorption of Pb(II), Cr(VI) ions and methylene blue to ACL and BCL had greater (r^2) values for PSO than PFO. Therefore, this implies that the removal mechanisms were mostly governed by chemisorption. The experimental (q_e) were also found to be closer to that of the calculated (q_e), further indicating that the removal mechanisms fitted PSO. The effect of agitation time data was also subjected to IPD model which explains the estimated pore filling (EPF) and estimated surface adsorption (ESP) onto the heterogeneous surface of the adsorbent. It was observed that the data well fitted this model with (r^2) values closer to 1. The data revealed that estimated surface adsorption (ESA) was prominent in most processes. However, estimated pore-filling (EPF) was dominant in the removal of Pb(II) ions and methylene blue onto PCL.

Effect of concentration: The effect of concentration of solution of Pb(II), Cr(VI) and methylene blue onto PCL, ACL and BCL was studied at varying initial concentrations within the range (20-200 mg/L). The plots are shown in Fig. 5a-c. It was observed that uptake by the adsorbents increased with increasing initial concentration of the solution. This could be explained by the fact that solutions with higher initial concentration such as 200 mg/L, has greater collision chances between Pb(II), Cr(VI) ions, methylene blue and the adsorbents surface and this is associated with higher mass transfer. The recorded adsorption capacities on solutions with initial concentration 200 mg/L were 69.42, 64.04, 64.88 mg/g for Cr(VI) ions, 39.36, 74.11, 78.34 for Pb(II) ions and 37.64, 46.28, 46.39 for methylene blue onto PCL, ACL and BCL, respectively.

Isotherm models: Table-2 shows the isotherm modelling of Langmuir and Freundlich which were intergraded into equilibrium data of Pb(II), Cr(VI) and methylene blue to determine the adsorption capacity and estimate the adsorption interaction

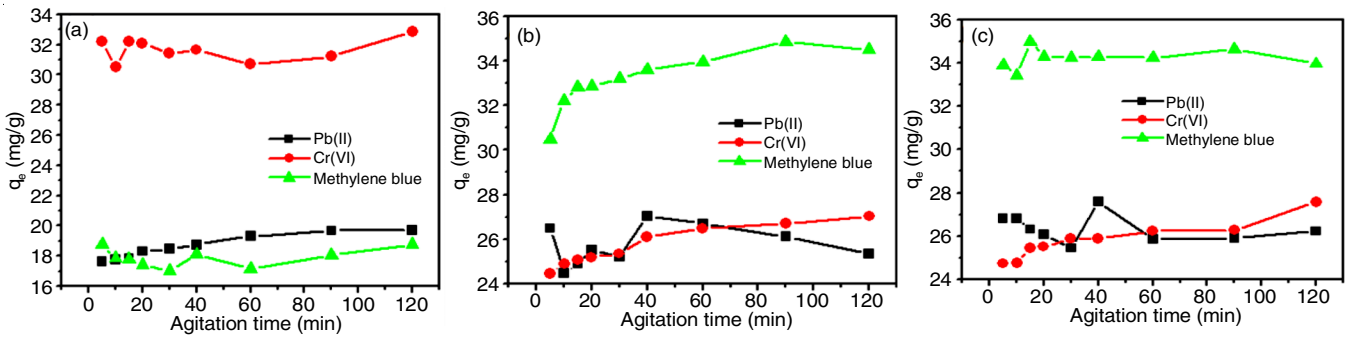

Fig. 4. Effect of agitation time for (a) PCL, (b) ACL and (c) BCL

TABLE-1
KINETIC MODELS FOR THE ADSORPTION OF Pb(II), Cr(VI) IONS AND METHYLENE BLUE ONTO PCL, ACL AND BCL

Kinetic model	Parameter	PCL			ACL			BCL		
		Pb(II)	Cr(VI)	Methylene blue	Pb(II)	Cr(VI)	Methylene blue	Pb(II)	Cr(VI)	Methylene blue
PFO	q_e (mg/g)	18.74	31.80	18.01	25.94	25.88	33.57	26.46	25.97	34.32
	k_1 (/min)	0.5421	0.624	0.456	0.558	0.566	0.464	0.624	0.581	0.724
	r^2	0.994	0.578	0.996	0.576	0.530	0.801	0.532	0.491	0.678
PSO	q_e (mg/g)	11.89	32.29	88.82	26.49	26.43	34.40	26.83	26.47	34.59
	k_2 (g/mg/min)	0.0504	0.084	0.010	0.070	0.0734	0.0427	0.111	0.0811	0.151
	r^2	0.9467	0.875	0.963	0.860	0.828	0.960	0.794	0.783	0.883
IPD	C (mg/g)	7.987	30.13	8.853	24.01	23.91	30.75	16.97	24.14	33.37
	k_i (g/g $min^{1/2}$)	0.6102	0.252	0.498	0.292	0.291	0.404	0.272	0.280	0.142
	r^2	0.9921	0.961	0.999	0.983	0.980	0.908	0.982	0.948	0.944
[1]EPF	%	60.01	8.34	52.79	11.18	11.54	10.87	38.49	12.51	4.61
[2]ESP	%	39.99	91.66	47.21	88.82	88.46	89.13	61.51	87.49	95.39
Experimental	q_e (mg/g)	19.71	32.87	18.76	27.03	27.03	34.50	27.59	27.59	34.98

[1]EPF (Estimated pore-filling) [2]ESP (Estimated surface adsorption)

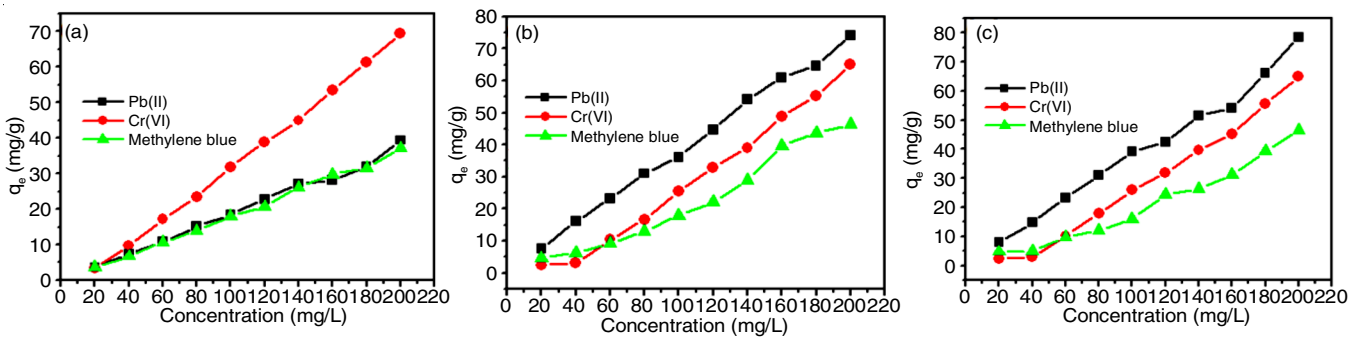

Fig. 5. Effect of concentration for (a) PCL, (b) ACL and (c) BCL

behaviour of PCL, ACL and BCL. It is observed from Table-2 that the uptake of Pb(II), Cr(VI) ions, methylene blue onto PCL fitted Freundlich the (r^2) values were between 0.926-0.998 close to the unity. Freundlich model suggests that the processes involved multi-layer adsorption interaction between the adsorbate and the adsorbent and this also implies heterogeneous nature of the adsorbent surface. Whilst the uptake of Cr(VI) ions and methylene blue onto ACL and BCL also fitted Freundlich. However, the uptake Pb(II) ions onto both onto ACL and BCL fitted Langmuir. The fits found with Langmuir model indicates that the adsorption took place on active sites having equal affinity for adsorbates and further suggests that monolayer adsorption occurred on adsorbents surface.

Effect of pH: The effect of solution pH was studied at (pH 2, 4, 6 8 and 10) as shown in Fig. 6a-c. It was observed from Fig. 6a that the uptake of Pb(II), Cr(VI) ions and methylene blue were pH dependent. The adsorption of Cr(VI) ions decreased with increasing pH of the solution. This could be explained by the fact that at low pH solution the surface of the adsorbent was protonated and acquired H^+ ions thus the negatively charged Cr(VI) ions existing as $HCrO_4^-$ were easily attracted to the active sites and the adsorption capacity was enhanced. Whilst at high pH of the solution the surface of the adsorbent was deprotonated hence the repulsive forces were increased between the $HCrO_4^-$ and the negatively charged surface thus adsorption capacity decreased. It was observed that the adsorption of Pb(II) and methylene blue steadily increased with increasing pH of the solution. The negatively charged surface easily attracted the positively charged Pb(II) ions and methylene blue. This helped to improve the forces of

TABLE-2
ISOTHERM MODELS FOR THE ADSORPTION OF Pb(II), Cr(VI) IONS AND METHYLENE BLUE ONTO PCL, ACL AND BCL

Isotherm	Parameter	PCL			ACL			BCL		
		Pb(II)	Cr(VI)	Methylene blue	Pb(II)	Cr(VI)	Methylene blue	Pb(II)	Cr(VI)	Methylene blue
Langmuir	Q_o (mg/g)	37.83	11.85	38.18	87.13	77.76	22.91	68.70	81.58	39.16
	β	0.0106	0.143	0.0729	1.122	0.0123	3.337	3.03	0.0115	6.315
	r^2	0.995	0.620	0.997	0.975	0.499	0.014	0.970	0.490	0.102
Freundlich	K_f	0.9795	0.041	0.963	41.57	5.18	0.477	40.43	0.0149	0.0174
	1/n	0.1679	0.143	0.150	3.11	0.156	0.472	5.32	0.165	0.434
	r^2	0.996	0.926	0.998	0.880	0.792	0.957	0.840	0.758	0.967
Experimental	q_e (mg/g)	39.36	69.42	37.24	74.11	65.04	46.28	78.34	64.88	46.39

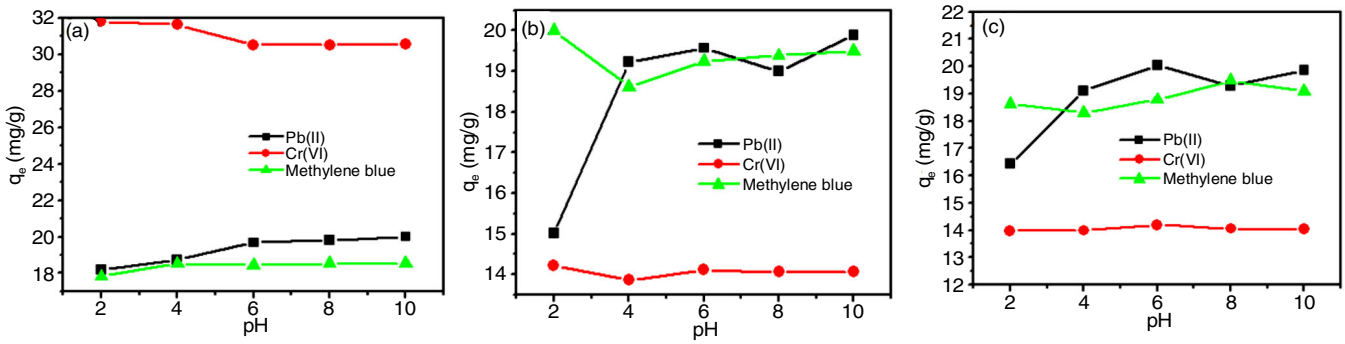

Fig. 6. Effect of pH for (a) PCL, (b) ACL and (c) BCL

attraction and the adsorption capacity. In Fig. 6b-c, the plots followed the same pattern. It was observed that the uptake of both Pb(II) ions and methylene blue onto ACL and BCL increased with increasing pH. Higher pH of the solution leads to deprotonation of the surface (*i.e.*) the surface has been dominated by negative charges, this resulted in enhanced adsorption. However, the adsorption of Cr(VI) ions as pH of the solution was increased resulted in a reduced uptake.

Effect of temperature on the adsorption of Pb(II) ions: The effect of temperature on the adsorption of Pb(II) ions onto PCL, ACL and BCL was evaluated at temperatures 298, 299 and 309 K with standard solutions 20, 40, 60, 80 and 100 mg/L as shown in Fig. 7a-c. It was observed that the adsorption of Pb(II) ions onto PCL in Fig. 7a showed that as temperature increases from 289 to 309 K it had little impact as the uptake showed a linear relationship for all the temperatures across all the concentrations. However in Fig. 7b-c, increasing the temperature from 298 to 299 K enhanced the uptake of Pb(II) ions onto ACL and BCL. This could be explained by the fact that slight increase in temperature to 299 K supplied the system with sufficient energy to overcome all hindering forces. Increase in temperature from 299 to 309 K favoured the uptake of Pb(II) which suggests that the reaction was endothermic in nature. However, further increase in temperature from 299 to 309 K was detrimental to adsorption of Pb(II) onto ACL. This suggests that at 309 K, Pb(II) ions in solution have gained enough kinetic energy in which they move rapidly resulting in less interaction with the adsorbent for adsorption to occur, hence low uptake is observed. This also suggests that the reaction was exothermic in nature.

Effect of temperature on the adsorption of Cr(VI) ions: The effect of temperature on the adsorption of Cr(VI) ions onto PCL, ACL and BCL was evaluated at 298, 299 and 309 K with standard solutions 20, 40, 60, 80 and 100 mg/L as shown in Fig. 8a-c. The plots revealed that the adsorption of Cr(VI) ions onto PCL in Fig. 8a showed that as temperature was increased from 289 to 309 K it had no impact on the pollutant uptake. However, in Fig. 8b-c, the plots revealed that when temperature was increased from 298 to 309 K it favoured the uptake of Cr(VI) ions onto ACL and BCL. This also suggests that the reaction was endothermic in nature.

Effect of temperature on the adsorption of methylene blue: The effect of temperature on the adsorption of methylene blue onto PCL, ACL and BCL was evaluated at temperatures 298, 299 and 309 K with standard solutions 20, 40, 60, 80 and 100 mg/L as shown in Fig. 9a-c. The plot for adsorption of Cr(VI) ions onto PCL in Fig. 9a showed that as temperature increased from 289 to 309 K it had no impact on the uptake of methylene blue. However, in Fig. 9b-c, the plots revealed that when temperature increased from 298 to 309 K it favoured the uptake of methylene blue onto ACL and BCL. This also suggests that the reaction was endothermic in nature.

Thermodynamic studies: The thermodynamic parameters; enthalpy (ΔH°), Gibbs free energy (ΔG°) and entropy (ΔS°) were evaluated at varying temperatures (298, 299 and 309 K) for Pb(II), Cr(VI) ions and methylene blue onto PCL, ACL and BCL as shown in Table-3. The data revealed that the adsorption of Pb(II) ions onto PCL and ACL and methylene blue dye onto PCL gave negative (ΔH°) values, this suggests that the reaction was an exothermic process. However, the adsorption of Pb(II) ion onto BCL gave positive (ΔH°), this suggests that the reaction is endothermic in nature, favouring adsorption of heat onto the system for a higher uptake. While the adsorption

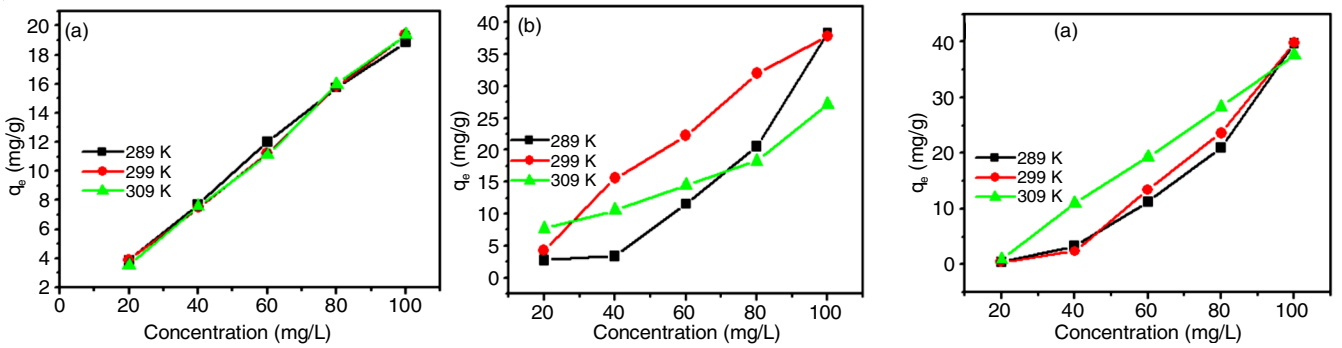

Fig. 7. Temperature effect for (a) PCL, (b) ACL and (c) BCL adsorption of Pb(II)

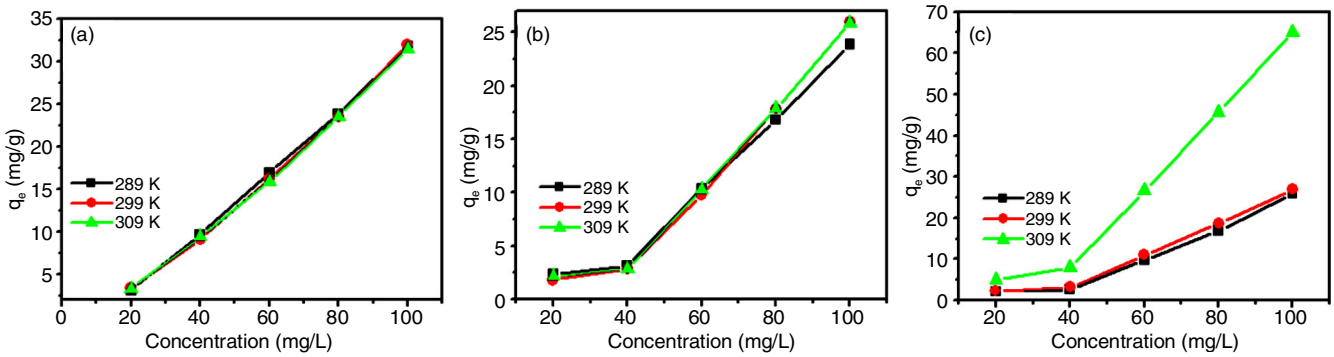

Fig. 8. Temperature effect of adsorption of Cr(VI) onto (a) PCL, (a) ACL and (c) BCL

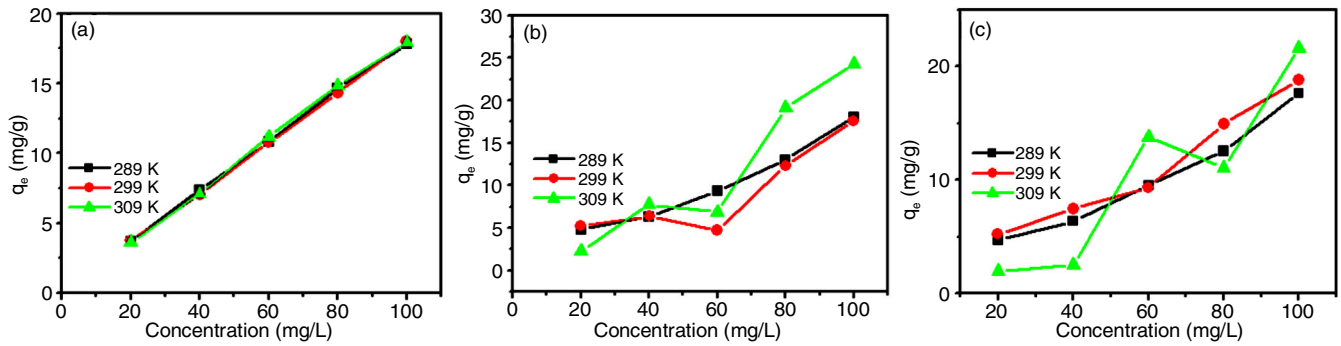

Fig. 9. Temperature effect for adsorption of methylene blue onto (a) PCL, (b) ACL and (c) BCL

of Cr(VI) ions and methylene blue gave positive (ΔH°) values, this indicated that the processes were endothermic in nature and increasing the temperature would enhance the uptake of Cr(VI) ions and methylene blue onto ACL and BCL. The obtained (ΔS°) values were all positive which indicated the randomness and degree of freedom for Pb(II), Cr(VI) ions and methylene blue in aqueous solution during the adsorption processes. The Gibb's free energy (ΔG°) gave negative values for the adsorption of Pb(II), Cr(VI) ions and methylene blue onto PCL, ACL and BCL at all studied temperatures in this study which implies that the processes were spontaneous

Conclusion

The effectiveness of PCL, ACL and BCL were evaluated for the uptake of Pb(II), Cr(VI) ions and methylene blue from aqueous solution. The morphology, functional groups and purity of the adsorbents were affirmed by SEM, FTIR and XRD, respectively. FTIR spectra affirmed the presence of (CO_3^{2-}) and (-C=O) groups of the carbonate ions attached onto surface PCL. Morphological analysis by SEM micrographs showed that the surface of all adsorbents was amorphous in nature and irregularly shaped. XRD spectra confirmed the orthorhombic structure of aragonite in the pristine coral limestones (PCL), acid modified coral limestones (ACL) and base modified coral limestones (BCL), with the modified adsorbents showing a lowered peak intensity. Batch adsorption parameters were carried while varying concentration, time, temperature and pH. The results revealed that adsorption of Pb(II), Cr(VI) ions and methylene blue was pH dependant. It was also found that adsorption capacity of PCL, ACL and BCL increased with increasing initial concentration Pb(II), Cr(VI) ions and methylene blue in the solution. The recorded maximum adsorption capacities of PCL, ACL and BCL for The recorded maximum adsorption capacities of PCL, ACL and BCL for Cr(VI) ions were 69.42, 65.04, 64.88 mg/g, Pb(II) ions 39.36, 74.11, 78.34 mg/g and methylene blue 37.24, 46.28, 46.39 mg/g, respectively. The data revealed that the adsorption of Pb(II) ions onto PCL and ACL was an exothermic reaction, however adsorption of Pb(II) ion onto BCL was endothermic. Whilst the adsorption of Cr(VI) ions and methylene blue were endothermic in nature

TABLE-3
THERMODYNAMICS STUDIES ON THE ADSORPTION OF Pb(II), Cr(VI) IONS AND METHYLENE BLUE

Thermodynamic parameter		PCL			ACL			BCL		
		Pb(II)	Cr(VI)	Methylene blue	Pb(II)	Cr(VI)	Methylene blue	Pb(II)	Cr(VI)	Methylene blue
ΔH° (kJ mol^{-1})		-18.48	14.47	-7.90	-23.96	5.22	2.72	12.26	4.06	2.98
ΔS° (J mol^{-1} K^{-1})		68.49	0.5742	20.40	76.38	1.432	8.23	41.07	13.64	6.70
ΔG° (kJ mol^{-1})	289 K	-3.617	-1.645	-2.780	-12.67	-0.919	-2.609	-2.332	-0.7115	-2.659
	299 K	-4.278	-1.786	-2.855	-15.11	-0.771	-2.815	-2.312	-2.677	-2.522
	309 K	-5.182	-1.648	-2.948	-0.426	-0.662	-1.162	-4.777	-1.597	-1.925

hence increasing the temperature would enhance the uptake of Cr(VI) ions and methylene blue onto ACL and BCL. The obtained (ΔG°) values for the adsorption of Pb(II), Cr(VI) ions and methylene blue onto PCL, ACL and BCL at all studied temperatures implies that the processes were spontaneous.

ACKNOWLEDGEMENTS

The authors acknowledge the supports of National Research Fund-NRF (TTK190403426819) for funding this work, the Department of Chemistry and Biotechnology, Vaal University of Technology, Vanderbijlpark, South Africa.

CONFLICT OF INTEREST

The authors declare that there is no conflict of interests regarding the publication of this article.

REFERENCES

1. S.E. Elaigwu, L.A. Usman, G.V. Awolola, G.B. Adebayo and R. Ajayi, *Environ. Res. J.*, **4**, 257 (2010); https://doi.org/10.3923/erj.2010.257.260
2. Z. Li, Z. Ma, T.J. van der Kuijp, Z. Yuan and L. Huang, *Sci. Total Environ.*, **468-469**, 843 (2014); https://doi.org/10.1016/j.scitotenv.2013.08.090
3. E. Iloms, O.O. Ololade, H.J.O. Ogola and R. Selvarajan, *Int. J. Environ. Res. Public Health*, **17**, 1096 (2020); https://doi.org/10.3390/ijerph17031096
4. D. Pathania, S. Sharma and P. Singh, *Arab. J. Chem.*, **10S**, S1445 (2017); https://doi.org/10.1016/j.arabjc.2013.04.021
5. N.D. Shooto, C.W. Dikio, D. Wankasi, L.M. Sikhwivhilu, F.M. Mtunzi and E.D. Dikio, *Nanoscale Res. Lett.*, **11**, 414 (2016); https://doi.org/10.1186/s11671-016-1631-2
6. A.T. Jan, M. Azam, K. Siddiqui, A. Ali, I. Choi and Q.M. Rizwanul Haq, *Int. J. Mol. Sci*., **16**, 29592 (2015); https://doi.org/10.3390/ijms161226183
7. X. Hu and X. Du, *Molecules*, **24**, 1449 (2019); https://doi.org/10.3390/molecules24081449
8. C. Qi, L. Xu, M. Zhang and M. Zhang, *Micropor. Mesopor. Mater.*, **290**, 109651 (2019); https://doi.org/10.1016/j.micromeso.2019.109651
9. E.O. Ezugbe and S. Rathilal, *Membranes*, **10**, 89 (2020); https://doi.org/10.3390/membranes10050089
10. Z. Aksu and F. Gonen, *Process Biochem.*, **39**, 599 (2004); https://doi.org/10.1016/S0032-9592(03)00132-8
11. R.K. Gautam, A. Mudhoo and M.C. Chattopadhyaya, *J. Environ. Chem. Eng.*, **1**, 1283 (2013); https://doi.org/10.1016/j.jece.2013.09.021
12. F.Y. Wang, H. Wang and J.W. Ma, *J. Hazard. Mater.*, **177**, 300 (2010); https://doi.org/10.1016/j.jhazmat.2009.12.032
13. C.S. Nkutha, P.N. Diagboya, F.M. Mtunzi and E.D. Dikio, *Water Environ. Res.*, **92**, 1070 (2020); https://doi.org/10.1002/wer.1303
14. J. Tao and A.M. Rappe, *Phys. Rev. Lett.*, **112**, 106101 (2014); https://doi.org/10.1103/PhysRevLett.112.106101
15. V.E. Pakade, T.D. Ntuli and A.E. Ofomaja, *Appl. Water Sci.*, **7**, 3015 (2017); https://doi.org/10.1007/s13201-016-0412-5
16. N.D. Shooto, P.M. Thabede and E.B. Naidoo, *South Afr. J. Chem. Eng.*, **30**, 15 (2019); https://doi.org/10.1016/j.sajce.2019.07.002
17. N.D. Shooto, C.S. Nkutha, N.R. Guilande and E.B. Naidoo, *South Afr. J. Chem. Eng.*, **31**, 33 (2020); https://doi.org/10.1016/j.sajce.2019.12.001
18. J. Abdulfatai, A.A. Saka, A.S. Afolabi and O. Micheal, *Appl. Mech. Mater.*, **248**, 310 (2012); https://doi.org/10.4028/www.scientific.net/AMM.248.310
19. S. Al-Rousan, R. Al-Shloul, F. Al-Horani and A. Abu-Hilal, *Environ. Earth Sci.*, **67**, 2003 (2012); https://doi.org/10.1007/s12665-012-1640-0
20. D.R. Mishra, S. Narumalani, D. Rundquist, M. Lawson and R. Perk, *J. Geophys. Res.*, **112**, C08014 (2007); https://doi.org/10.1029/2006JC003892
21. S. Reza, E.H. Reza and T.A. Monire, *J. Environ. Technol. Sci.*, **16**, 109 (2012).
22. R. Shokoohi, M.T. Samadi, M.R. Samarghandi, M. Ahmadian, K. Karimaian and A. Poormohammadi, *Saudi J. Biol. Sci.*, **24**, 749 (2017); https://doi.org/10.1016/j.sjbs.2016.01.012
23. R. Nourozi, M.T. Samadi and M.H. Mehdinejad, *J. Health Environ.*, **5**, 479 (2012).
24. M. Malakootian, S. Mohammad, N. Amirmahani, Z. Nasiri and A. Nasiri, *J. Commun. Health Res.*, **5**, 73 (2016).
25. Y. Du, F. Lian and L. Zhu, *Environ. Pollut.*, **159**, 1763 (2011); https://doi.org/10.1016/j.envpol.2011.04.017
26. B. Kaczorowska, A. Hacura, T. Kupka, R. Wrzalik, E. Talik, G. Pasterny and A. Matuszewska, *Anal. Bioanal. Chem.*, **377**, 1032 (2003); https://doi.org/10.1007/s00216-003-2153-1
27. J. Balmain, B. Hannoyer and E. Lopez, *Biomed. Mater. Res.*, **48**, 749 (1999); https://doi.org/10.1002/(SICI)1097-4636(1999)48:5<749::AID-JBM22>3.0.CO;2-P